R. & M. No. 3643

R. & M. No. 3643

MINISTRY OF TECHNOLOGY

AERONAUTICAL RESEARCH COUNCIL

REPORTS AND MEMORANDA

Improved Entrainment Method for Calculating Turbulent Boundary Layer Development

By M. R. HEAD and V. C. PATEL

Cambridge University Engineering Department

LONDON: HER MAJESTY'S STATIONERY OFFICE

1970

PRICE 14*s* 0*d* [70p] NET

Improved Entrainment Method for Calculating Turbulent Boundary Layer Development

By M. R. HEAD and V. C. PATEL
Cambridge University Engineering Department

Reports and Memoranda No. 3643*
March, 1968

Summary.

A simple integral method is presented for the calculation of two-dimensional incompressible turbulent boundary layers.

Use is made of established relationships to determine values of the entrainment coefficient for equilibrium layers, and the entrainment coefficient for non-equilibrium conditions is obtained by multiplying the corresponding equilibrium value by a suitable empirical function. This increases the entrainment when the rate of growth of the layer is less than that of the corresponding equilibrium layer, and decreases it when the rate of growth is greater. This variation of entrainment is in accordance with observation, and a simple physical explanation is proposed to account for it. This explanation further suggests how the effects of flow convergence may be taken into account.

Comparisons with measured boundary-layer developments show the general accuracy of the method.

LIST OF CONTENTS

*Replaces A.R.C. 31 043.

---

1. *Introduction.*

At a recent symposium held at Stanford[4], some thirty different methods of calculating the development of the turbulent boundary layer were compared and assessed. Most of the methods had been developed comparatively recently and some showed very satisfactory agreement with at least a majority of the wide range of experimental data against which the calculations were tested. Among the most successful methods, those of Bradshaw, Nash and Felsch are probably worthy of mention. An early method due to one of the present authors[3] showed up reasonably satisfactorily and was placed in the middle third, and it is a development of this method that is presented here. As it now stands the method would appear to be at least as accurate as the best presented at Stanford while being sufficiently simple to enable a hand calculation to be completed in an hour or two, and a computer calculation in a very few seconds.

Although the modifications to the original method were arrived at largely empirically, some justification on physical grounds can be provided, as will be seen later. A brief account of the development of the present method is given in the following sections. Comparisons with experiment are presented towards the end of the report.

2. *The Original Entrainment Method.*

In this, the very simple assumption was made that the rate at which free-stream fluid was incorporated into the boundary layer was determined by the velocity defect in the outer part of the layer, and two measured boundary-layer developments were analysed and used to relate the non-dimensional rate of entrainment to the boundary layer form parameter $H^*\left(\equiv \frac{\delta-\delta^*}{\theta}\right)$. The same sets of measurements were used to relate H^* to the more conventional form parameter $H\left(\equiv \frac{\delta^*}{\theta}\right)$. Thus, the non-dimensional entrainment rate C_E was given by

$$C_E = \frac{1}{U}\frac{dQ}{dx} = \frac{1}{U}\frac{d}{dx}[\,U(\delta-\delta^*)\,] = F(H^*)$$

$$\text{and } H^* = G(H).$$

The two functions F and G were presented as curves which could be approximated by simple analytic expressions for computer calculations.

It will be seen that the functions F and G serve as an auxiliary equation for the calculation of H development. If the value of H^* is known at any point, the non-dimensional entrainment is also known, and from this the increment in $U(\delta-\delta^*)$ over a step can be obtained. The momentum integral equation gives a corresponding increment in $U\theta$, and the values of $U(\delta-\delta^*)$ and $U\theta$ at the end of the step give the value of H^* there, and hence the corresponding value of H, which enables the calculation to proceed.

3. *Shortcomings of the Original Method.*

The assumption that the entrainment is uniquely related to the boundary-layer form parameter is obviously likely to prove an over-simplified one, and it is perhaps surprising that it gives satisfactory results in quite a wide range of cases, including, in particular, layers with injection. Where the method does fall down is in the case of equilibrium flows and flows where a strong adverse pressure gradient is followed by a region of zero pressure gradient. In both these cases the trends are correctly predicted but actual magnitudes are appreciably in error. For example, the method would predict a value of H of approximately 1·8 for Bradshaw's equilibrium flow $a = -0{\cdot}255$, as compared to the measured value of approximately 1·59, and when this adverse pressure gradient is followed by a region of constant pressure, the value of H tends to the zero pressure gradient value, but much too slowly.

4. *Development of the Present Method.*

The foregoing observations, if closely examined, are sufficient to suggest that, if the entrainment in the equilibrium layer is taken as datum, then, for layers proceeding to separation, the entrainment should be reduced, and for layers where H is decreasing it should be increased.

We can secure this result by multiplying C_E for the equilibrium layer by a suitable function of some parameter that measures the departure from equilibrium conditions. There are a large number of parameters that could be used for this purpose; the one actually chosen is the ratio $\frac{1}{U}\frac{d(U\theta)}{dx} \bigg/ \left[\frac{1}{U}\frac{d(U\theta)}{dx}\right]_{eq}$ for which we use the symbol r_1. If $r_1 = 1$ then we have equilibrium conditions; if $r_1 > 1$ then we have a layer with R_θ increasing more rapidly than in the equilibrium case, and H increasing; if $r_1 < 1$ we have a layer with R_θ increasing less rapidly than in the equilibrium case, and H decreasing.

We therefore write $C_E = (C_E)_{eq}\,F(r_1)$, where $(C_E)_{eq}$ is the entrainment coefficient for the equilibrium layer and $F(r_1)$ is a function that must satisfy the following conditions.

(i) For $r_1 = 1$ (i.e. equilibrium conditions) $F(r_1) = 1$.

(ii) For $r_1 > 1$ (i.e. layers with R_θ growing more rapidly than the corresponding equilibrium layer) $F(r_1) < 1$, but however large r_1 becomes $F(r_1)$ must remain positive, since there is no reason to expect that the entrainment should become negative in a boundary layer that is growing rapidly.

(iii) For $r_1 < 1$ (i.e. layers with R_θ growing less rapidly than the corresponding equilibrium layer) $F(r_1) > 1$, but however small, or even negative, r_1 should become, $F(r_1)$ should remain finite and probably not greater than (say) 2.

Now, a simple function that satisfies these requirements is shown in Fig. 1. This particular function was chosen quite arbitrarily, and although a more suitable function may well exist, there is no indication from the calculations so far performed that this should be the case.

With the function $F(r_1)$ determined, C_E can be found for given values of H and R_θ if $(C_E)_{eq}$ is known as function of these variables. In equilibrium layers, H and H^* vary only slowly with x and we can therefore write

$$(C_E)_{eq} = \frac{1}{U}\frac{d}{dx}\Big[U(\delta-\delta^*)\Big]_{eq} = \frac{1}{U}\frac{d}{dx}\Big[H^*(U\theta)\Big]_{eq} = H^*\left[\frac{1}{U}\frac{d(U\theta)}{dx}\right]_{eq}. \tag{1}$$

Further, $\left[\frac{1}{U}\frac{d(U\theta)}{dx}\right]_{eq}$ can readily be found from the $\pi - G$ relation given by Nash[5] by making use of the momentum integral equation and a skin-friction relation such as that given by Thompson[6] and shown in Fig. 2.

$\left[\frac{1}{U}\frac{d(U\theta)}{dx}\right]_{eq}$ is shown as a function of H and R_θ in Fig. 3.

To complete the calculation method all that is required is a relation between H^* and H, and this is provided by Thompson's profile family[6], δ being taken for the present purpose as the value of y for which $\frac{u}{U} = 0{\cdot}995$. H^* is shown as a function of H and R_θ in Fig. 4.

The only further point to be remarked is that, instead of using equation (1), it may be somewhat more convenient to use an equation giving the rate of change of H^* explicitly. Thus

$$\theta\frac{dH^*}{dx} = H^*\left[\frac{1}{U}\frac{d(U\theta)}{dx}\right]_{eq}\left[F(r_1)-r_1\right]. \tag{2}$$

The derivation of equation (2) and details of the procedure used to determine $\left[\frac{1}{U}\frac{d(U\theta)}{dx}\right]_{eq}$ are given in the Appendix.

The method may now be described as follows.

The momentum integral equation is used in the form

$$\frac{1}{U}\frac{d(U\theta)}{dx} = \frac{c_f}{2}-(H+1)\frac{\theta}{U}\frac{dU}{dx} \tag{3}$$

to find the increment in $U\theta$ over a step.

The value of r_1 is obtained from equation (3) and the corresponding value of $\left[\frac{1}{U}\frac{d(U\theta)}{dx}\right]_{eq}$. $F(r_1)$ is obtained from the value of r_1 and H^* is known from the values of H and R_θ. Equation (2) can thus be used to find the increment in H^*.

The values of H^* and R_θ at the end of the step give the value of H and the calculation can proceed.

For hand calculations we use Figs. 1, 2 and 3 and 4.

For computer calculations Fig. 1 is replaced by the relations

$$F(r_1) = \frac{1}{2r_1-1} \quad \text{for} \quad r_1 \geqslant 1,$$

$$\text{and} \quad F(r_1) = \frac{5-4r_1}{3-2r_1} \quad \text{for} \quad r_1 < 1,$$

Fig. 2 may be approximated by the analytic relation

$$c_f = \exp{(a\,H+b)}$$

$$\text{where} \quad a = 0{\cdot}019521-0{\cdot}386768c+0{\cdot}028345c^2-0{\cdot}000701c^3$$

$$b = 0{\cdot}191511-0{\cdot}834891c+0{\cdot}062588c^2-0{\cdot}001953c^3$$

$$\text{and} \quad c = \log_e R_\theta$$

and Fig. 3 is replaced by the use of equations A.1, A.2 and A.3 given in the Appendix. It is still necessary, however, to store Fig. 4, and in Table 1 values of $H(H^*, R_\theta)$ are given at sufficiently close intervals for linear interpolation to be used with acceptable accuracy.

5. *Physical Considerations.*

It is well established that the outer part of the turbulent boundary layer consists of a series of billows or clumps or eddies of turbulent fluid (*see*, for example, Fig. 1 in Reference 2). It is the existence of these that is responsible for the phenomenon of intermittency. Smoke observations show that the billows (as we shall call them) are essentially three-dimensional in character, with a cross-stream dimension that is generally similar to that in the streamwise direction. Since the outer boundary of the turbulent flow is normally defined by the outer boundaries of these billows, it seems reasonable to suppose that the closeness with which they are packed will define the distribution of intermittency; the closer the packing (in terms of boundary-layer thickness) the narrower the spread of intermittency and the more it will be confined to the region of small velocity defect close to the boundary-layer edge.

In an equilibrium layer, we should expect an equilibrium spacing of billows, and a corresponding distribution of intermittency, which, in terms of boundary-layer thickness should be largely independent of Reynolds number, though it may be expected to depend upon the value of the pressure gradient parameter π.

Now, any retardation of the flow beyond that occurring in equilibrium conditions will lead to a closer packing of the billows and hence a reduction in the spread of intermittency, while any relaxation will lead to a wider spacing and hance an increased spread of intermittency. It is to be expected that, for a given distribution of mean velocity in the outer part of the layer (i.e. a given value of H), these changes in the distribution of intermittency will be reflected in corresponding changes in the entrainment.

By whatever mechanism the entrainment of free-stream fluid is assumed to occur, it would seem that it must be reduced if the intermittency distribution is confined to a narrow region of small velocity defect, and increased by the presence of a more irregular boundary, which pentrates more deeply into the layer.

We may then reasonably assume that the packing of the billows and the resulting distribution of intermittency will have an important effect on the entrainment, over and above that exerted by the defect of mean velocity in the outer part of the layer. The ratio r_1 may be taken as a measure of the closeness of this packing.

The foregoing account of the role played by the packing of billows is, of course, purely speculative but it has some degree of plausibility and accords with observations of the smoke-filled boundary layer. Certain aspects of the present hypothesis can readily be checked by making measurements of intermittency in a variety of situations, and it is hoped to undertake such an investigation in the future.

From the arguments outlined above we may also deduce that convergence of the flow will increase the closeness of packing of the billows and hence reduce the entrainment, while divergence of the flow will have the opposite effect. This suggestion forms the basis for the extension of the present calculation method described in the next section.

6. *Extension of the Calculation Method to deal with Three-Dimensional Effects.*

It is comparatively seldom that boundary-layer developments have been measured in accurately two-dimensional conditions, as reference to the Stanford data shows. Some measure of flow convergence or divergence is almost invariably present in the experiment, leading to rates of boundary-layer growth that are respectively greater and less than would be obtained in two-dimensional conditions.

At the end of the previous section it was suggested that flow convergence should lead to a reduction of entrainment and that divergence should lead to an increase. We now make the tentative assumption that the influence of convergence on entrainment is precisely similar to that of an increased rate of growth in two-dimensional conditions. In other words, the same parameter $\frac{1}{U}\frac{d(U\theta)}{dx}\Big/\left[\frac{1}{U}\frac{d(U\theta)}{dx}\right]_{eq}$ is used as a measure of the entrainment for given values of H and R_θ, $\frac{1}{U}\frac{d(U\theta)}{dx}$ now representing the rate of growth in conditions of flow convergence or divergence. This very simple assumption leads, as we shall see, to predictions of H development that are in very much better agreement with experiment than predictions based on the assumption of two-dimensional conditions.

The following shows the modifications to the equations required to take account of observed departures from two-dimensionality. If we assume that such departures are confined to pure convergence or divergence the momentum integral equation becomes

$$\frac{1}{U}\frac{d(U\theta)}{dx} = \frac{c_f}{2} - (H+1)\frac{\theta}{U}\frac{dU}{dx} - \frac{\theta}{x-x_0}, \tag{4}$$

where x_0 represents the distance from the origin to the point of convergence of the external streamlines. For divergent flow $x-x_0$ is positive; for convergent flow it is negative. In general, x_0 may be expected to vary with x.

The entrainment equation is now given by

$$\frac{1}{U}\frac{d}{dx}[U(\delta-\delta^*)] = C_E - H^*\frac{\theta}{x-x_0}. \tag{5}$$

From the definition of H^* it is readily shown that

$$\theta\frac{dH^*}{dx} = \frac{1}{U}\frac{d}{dx}[U(\delta-\delta^*)] - \frac{H^*}{U}\frac{d(U\theta)}{dx}.$$

Substituting from (4) and (5) we then have

$$\theta\frac{dH^*}{dx} = C_E - H^*\left[\frac{1}{U}\frac{d(U\theta)}{dx}\right]_{2D},$$

where $$\left[\frac{1}{U}\frac{d(U\theta)}{dx}\right]_{2D} = \frac{c_f}{2} - (H+1)\frac{\theta}{U}\frac{dU}{dx}.$$

It will be noted that the convergence terms have disappeared.

From the suggestion made above, that the effect of convergence on entrainment should be adequately accounted for by treating the additional rate of growth as though it arose from normal two-dimensional causes, the entrainment coefficient is now given by

$$C_E = H^*\left[\frac{1}{U}\frac{d(U\theta)}{dx}\right]_{eq} F(r_2), \tag{6}$$

where $$r_2 \text{ is the ratio} \left[\frac{1}{U}\frac{d(U\theta)}{dx}\right]_{\text{expt}} \Big/ \left[\frac{1}{U}\frac{d(U\theta)}{dx}\right]$$

Hence, $$\theta\frac{dH^*}{dx} = H^*\left[\frac{1}{U}\frac{d(U\theta)}{dx}\right]_{eq}\left[F(r_2) - r_1\right]. \tag{7}$$

Thus, in conditions where the development of θ is known, we need not find explicitly the flow convergence or divergence at each point but only the experimental values of $\frac{1}{U}\frac{d(U\theta)}{dx}$. Two-dimensional values of the same quantity, required to determine r_1, follow from the values of H and R_θ and the pressure gradient at any point.

In any particular case, then, where the experimental development of θ does not satisfy the two-dimensional momentum integral equation we may use equation (7) in place of equation (3), feeding into the calculation the measured $U\theta$ development in place of the assumption of two-dimensionality.

It may readily be shown that, when we use the measured θ development as the basis for our calculation of H, there is no point in recalculating the θ development (except, possibly, as a check on the computation procedure); the use of the momentum integral equation with calculated values of H and c_f, and convergence or divergence terms corresponding to them, should simply lead to the measured θ development being reproduced.

This would not be precisely the case if we fed into the H calculations values of convergence or divergence determined from the use of measured H and c_f values, and it would then seem necessary to recalculate the θ development.

In the calculations to be described, the simpler procedure outlined above has been adopted wherever it has been thought worthwhile to take three-dimensionality into account. Thus, the calculated and experimental θ development for these cases automatically coincide.

7. *Cases Treated.*

A considerable range of cases has been considered and a representative selection of results is shown here. Three basically different types of flow have been treated:

(i) *Equilibrium flows.*
Bradshaw ($a = -0{\cdot}255$)
Bradshaw ($a = -0{\cdot}15$)
Herring and Norbury ($\beta = -0{\cdot}35$)

(ii) *Separating flows.*
Schubauer and Spangenberg A
Schubauer and Spangenberg E
Schubauer and Spangenberg B
Schubauer and Klebanoff
Ludwieg and Tillman
(strong adverse pressure gradient)
Goldberg 6

(iii) *Flows with H decreasing*
Tillmann (reattaching flow)
Bradshaw's relaxing layer
Goldberg 3

The results are shown in Figs. 5 to 16 with (in some cases) the results of Bradshaw, Ferriss and Atwell[1] included for comparison*. For most of the cases both two-dimensional and three-dimensional calculations were performed.

In only one case, that of Goldberg 3, has any modification been made to the procedure described in earlier sections. In this case, where H first rises rapidly, then falls, agreement with experiment is greatly improved if we introduce an expression which limits the rate of change of C_E, in other words if we relax the stringent coupling we have imposed between C_E and local conditions. The expression we have used is

$$\Delta C_E = \frac{\Delta C_{E\,\mathrm{nom}}}{1 + 400\,\Delta C_{E\,\mathrm{nom}} \dfrac{\theta}{\Delta x}},$$

where ΔC_E is the change of entrainment coefficient over the step length Δx, and $\Delta C_{E\,\mathrm{nom}}$ is the change in C_E that would follow from the use of equation (1) or (6) at the beginning and end of the step. The use of this expression, which was introduced at a fairly late stage, appears to have a negligible effect on the flows calculated earlier.

---

*The authors are indebted to Mr. P. Bradshaw for providing detailed results of the calculations.

8. *Discussion.*

From an examination of Figs. 5 to 16 three points emerge very clearly.

First, it is apparent that, where the flow is closely two-dimensional, as evidenced by the agreement between the measured θ development and that obtained from the two-dimensional calculation, the predicted H development is also in good agreement with the measurements (*see*, for example, Figs. 5, 6, 8, 9, 13 and 15).

Second, where departures from two-dimensionality are small, the use of the three-dimensional correction may convert agreement which is merely satisfactory to agreement which is very nearly perfect (*see*, for example, Figs. 5, 6, 7 and 10). Where there are gross departures from two-dimensionality, the three-dimensional correction appears always to operate in the correct sense, though the final agreement may still not be completely satisfactory. (*See* Figs. 11 and 12). The possibility cannot of course be dismissed that in these cases factors other than simple flow convergence or divergence may be operative. For example, the stabilising influence of surface curvature in the flow measured by Schubauer and Klebanoff may well result in a reduction of entrainment that is not considered here, though Thompson[7] has indicated how such an effect might be taken into account.

Taken overall there can be little doubt that the present correction for convergence or divergence makes a useful contribution to the calculation of nominally two-dimensional layers and may have important implications for the calculation of three-dimensional layers.

Finally, from the comparisons with the calculations by Bradshaw *et al* it appears that the latter are fairly consistently in error in the prediction of skin friction, and, in this respect at least, the present method is clearly superior.

As a general comment it may be said that the comparisons with experiment confirm the validity of the assumption that in two-dimensional flow C_E is determined by local values of H, R_θ and $\frac{\theta}{U}\frac{dU}{dx}$, which is the basic assumption of the present method. Only in the case of Goldberg 3 (Fig. 16) is the validity of this assumption seriously open to question. In this particular case, where $\frac{\theta}{U}\frac{dU}{dx}$ and H change very rapidly, the introduction of an expression which tends to limit the rate of change of C_E brings the calculations into satisfactory agreement with the measurements, but whether this particular axisymmetric experiment is sufficiently accurate and representative of two-dimensional conditions to justify the precise form of this correction is open to question. If this type of pressure distribution is of practical significance, then accurate two-dimensional experiments are certainly called for.

9. *Conclusions.*

The method of calculation presented here has been shown to give very satisfactory agreement with experiment in a wide variety of flow situations.

The proposed method of taking into account the effects of flow convergence and divergence has been shown to produce a very considerable improvement in the general accuracy of prediction.

It is evident from the present results that methods which do not take the history of the layer explicitly into account (except in so far as this is reflected in local values of H and R_θ) may yet be capable of giving accurate results in a very wide variety of conditions, and the speed and simplicity of the present method should make it attractive for many applications. Computing times on the Cambridge Titan computer are of the order of one to five seconds.

Acknowledgements.

Preliminary work on the present method was undertaken while the first author was working as vacation ment of Dr. J. J. Cornish and the assistance of Mr. J. Halligan. The report was revised while the first author was Visiting Professor at IIT Kanpur, India.

REFERENCES

No.	Author(s)	Title, etc.
1	P. Bradshaw, D. H. Ferriss and N. P. Atwell ..	Calculation of boundary-layer development using the turbulent energy equation. J. Fluid Mech. Vol. 28, p. 593. 1967.
2	H. Fiedler and M. R. Head ..	Intermittency measurements in the turbulent boundary layer. J. Fluid Mech. Vol. 25, p. 719. 1966.
3	M. R. Head	Entrainment in the turbulent boundary layer. A.R.C. R. & M. 3152. 1958.
4	S. J. Kline, H. K. Moffatt and M. V. Morkovin	Report on the AFOSR-IFP-Stanford Conference on computation of turbulent boundary layers. J. Fluid Mech. Vol. 36, p. 481. 1969.
5	J. F. Nash	Turbulent boundary-layer behaviour and the auxiliary equation. A.R.C. C.P. 835. 1965.
6	B. G. J. Thompson	A new two-parameter family of mean velocity profiles for incompressible boundary layers on smooth walls. A.R.C. R. & M. 3463. 1965.
7	B. G. J. Thompson	The calculation of shape-factor development in incompressible turbulent boundary layers with or without transpiration. AGARDograph 97, p. 159. 1965.

APPENDIX

(i) *Determination of* $\left[\frac{1}{U}\frac{d(U\theta)}{dx}\right]_{eq}$

Nash[5] gives the following expression relating π and G for equilibrium layers

$$G = 6{\cdot}1\,(\pi+1{\cdot}81)^{\frac{1}{2}}-1{\cdot}7,$$

where

$$\pi = \frac{\delta^*}{\tau_w}\frac{dp}{dx}$$

and

$$G = \frac{H-1}{H}\left(\frac{2}{c_f}\right)^{\frac{1}{2}}. \tag{A.1}$$

This expression may be written

$$\pi = \left[\frac{G+1{\cdot}7}{6{\cdot}1}\right]^2-1{\cdot}81. \tag{A.2}$$

From the momentum integral equation we have

$$\frac{1}{U}\frac{d(U\theta)}{dx} = \frac{c_f}{2}\left[1-(H+1)\frac{2}{c_f}\frac{\theta}{U}\frac{dU}{dx}\right],$$

$$= \frac{c_f}{2}\left[1+\frac{H+1}{H}\frac{\delta^*}{\tau_w}\frac{dp}{dx}\right].$$

Hence

$$\left[\frac{1}{U}\frac{d(U\theta)}{dx}\right]_{eq} = \frac{c_f}{2}\left[1+\frac{H+1}{H}\pi\right]. \tag{A.3}$$

For given values of H and R_θ we can obtain c_f, and hence G from (A.1), and the corresponding value of π from (A.2). $\left[\frac{1}{U}\frac{d(U\theta)}{dx}\right]_{eq}$ then follows from (A.3).

(ii) *Derivation of equation* (2) *in main text.*

$$\theta\frac{dH^*}{dx} = \theta\frac{d}{dx}\left[\frac{U(\delta-\delta^*)}{U\theta}\right] = \frac{1}{U}\frac{d}{dx}[U(\delta-\delta^*)] - \frac{\delta-\delta^*}{\theta}\frac{1}{U}\frac{d(U\theta)}{dx}$$

$$= C_E - H^*\frac{1}{U}\frac{d(U\theta)}{dx}$$

$$= (C_E)_{eq}F(r_1) - H^*\frac{1}{U}\frac{d(U\theta)}{dx}$$

$$= H^*\left[\frac{1}{U}\frac{d(U\theta)}{dx}\right]_{eq}[F(r_1)-r_1].$$

TABLE 1

$H(H^*, R_\theta)$
$2{\cdot}5 \leqslant \log_{10} R_\theta \leqslant 3{\cdot}2$

$\mathrm{Log}_{10} R_\theta$	2·500	2·600	2·700	2·800	2·900	3·000	3·100	3·200
H^*								
3·600	0	0	0	0	0	0	0	0
3·650	0	0	0	0	0	0	0	0
3·700	0	0	0	0	0	0	0	0
3·750	0	0	0	0	0	0	0	0
3·800	0	0	0	0	0	0	0	0
3·850	0	0	0	0	0	0	2·795	2·635
3·900	0	0	0	0	2·800	2·640	2·545	2·460
3·950	0	0	2·800	2·620	2·515	2·450	2·380	2·330
4·000	0	2·655	2·540	2·450	2·375	2·320	2·270	2·235
4·100	2·500	2·400	2·330	2·280	2·230	2·180	2·115	2·085
4·200	2·340	2·275	2·220	2·170	2·125	2·090	2·055	2·025
4·300	2·260	2·195	2·135	2·090	2·050	2·020	1·985	1·955
4·400	2·185	2·130	2·085	2·040	2·005	1·965	1·940	1·915
4·600	2·085	2·030	1·985	1·950	1·915	1·880	1·855	1·830
4·800	2·010	1·960	1·910	1·880	1·845	1·810	1·780	1·750
5·000	1·960	1·905	1·865	1·825	1·795	1·765	1·725	1·700
5·500	1·885	1·795	1·750	1·715	1·675	1·650	1·625	1·600
6·000	1·840	1·735	1·695	1·655	1·625	1·590	1·565	1·540
6·500	1·750	1·700	1·655	1·620	1·585	1·555	1·525	1·495
7.000	1·725	1·670	1·625	1·590	1·555	1·525	1·490	1·470
8·000	1·675	1·625	1·580	1·540	1·505	1·480	1·455	1·435
9·000	1·635	1·580	1·535	1·495	1·460	1·435	1·405	1·385
1·000*1	1·590	1·535	1·485	1·450	1·420	1·395	1·365	1·345
1·000*1	1·545	1·485	1·445	1·415	1·380	1·355	1·335	1·320
1·200*1	1·505	1·455	1·415	1·385	1·355	1·330	1·305	1·285
1·300*1	1·470	1·425	1·390	1·355	1·325	1·295	1·270	1·250
1·400*1	1·430	1·390	1·350	1·320	1·290	1·270	1·245	1·230

TABLE 1—*continued*

$H(H^*, R_\theta)$
$3{\cdot}3 \leqslant \log_{10} R_\theta \leqslant 4{\cdot}0$

$\mathrm{Log}_{10}\, R_\theta$	3·300	3·400	3·500	3·600	3·700	3·800	3·900	4·000
3·600	0	0	0	0	0	0	0	0
3·650	0	0	0	0	0	0	0	0
3·700	0	0	0	0	0	0	2·850	2·605
3·750	0	0	2·835	2·680	2·590	2·510	2·450	2·405
3·800	2·795	2·665	2·565	2·480	2·425	2·370	2·330	2·290
3·850	2·555	2·480	2·415	2·360	2·315	2·265	2·235	2·200
3·900	2·395	2·340	2·290	2·250	2·215	2·185	2·150	2·120
3·950	2·290	2·250	2·210	2·180	2·145	2·115	2·090	2·070
4·000	2·195	2·165	2·135	2·105	2·085	2·060	2·045	2·025
4·100	2·060	2·035	2·015	1·995	1·975	1·955	1·940	1·910
4·200	2·000	1·975	1·955	1·935	1·915	1·900	1·875	1·870
4·300	1·935	1·915	1·890	1·875	1·860	1·845	1·835	1·820
4·400	1·890	1·865	1·850	1·830	1·815	1·800	1·790	1·775
4·600	1·805	1·785	1·765	1·745	1·735	1·720	1·705	1·700
4·800	1·725	1·700	1·670	1·660	1·650	1·635	1·630	1·620
5·000	1·675	1·655	1·635	1·620	1·610	1·600	1·585	1·580
5·500	1·575	1·560	1·540	1·525	1·510	1·500	1·485	1·480
6·000	1·520	1·500	1·480	1·465	1·455	1·440	1·435	1·420
6·500	1·475	1·455	1·440	1·425	1·415	1·405	1·395	1·385
7·000	1·445	1·430	1·415	1·400	1·385	1·375	1·370	1·360
8·000	1·415	1·395	1·380	1·365	1·350	1·340	1·330	1·325
9·000	1·365	1·350	1·340	1·325	1·315	1·305	1·295	1·290
1·000*1	1·330	1·320	1·310	1·295	1·285	1·280	1·270	1·265
1·000*1	1·305	1·290	1·280	1·270	1·260	1·250	1·245	1·240
1·200*1	1·270	1·255	1·245	1·235	1·230	1·225	1·220	1·215
1·300*1	1·235	1·220	1·210	1·205	1·195	1·190	1·190	1·185
1·400*1	1·215	1·205	1·190	1·185	1·180	1·175	1·170	1·170

TABLE 1—*continued*

$H(H^*, R_\theta)$
$4{\cdot}2 \leqslant \log_{10} R_\theta \leqslant 5{\cdot}4$

$\text{Log}_{19} R_\theta$	4·200	4·400	4·600	4·800	5·000	5·200	5·400
H*							
3·600	0	0	0	0	0	2·764	2·640
3·650	0	2·665	2·535	2·455	2·405	2·365	2·330
3·700	2·490	2·415	2·350	2·305	2·270	2·245	2·230
3·750	2·330	2·270	2·225	2·19	2·170	2·150	2·140
3·800	2·230	2·180	2·145	2·120	2·095	2·080	2·070
3·850	2·145	2·110	2·075	2·050	2·035	2·025	2·015
3·900	2·075	2·040	2·015	1·995	1·980	1·975	1·970
3·950	2·025	1·995	1·975	1·955	1·845	1·935	1·930
4·000	1·985	1·960	1·935	1·920	1·905	1·895	1·890
4·100	1·885	1·865	1·850	1·840	1·835	1·835	1·830
4·200	1·850	1·830	1·815	1·805	1·795	1·790	1·785
4·300	1·800	1·785	1·775	1·765	1·760	1·750	1·745
4·400	1·760	1·745	1·730	1·720	1·715	1·710	1·705
4·600	1·680	1·670	1·660	1·655	1·650	1·650	1·645
4·800	1·610	1·605	1·600	1·595	1·595	1·590	1·590
5·000	1·565	1·555	1·550	1·545	1·540	1·540	1·540
5·500	1·465	1·460	1·450	1·450	1·450	1·445	1·445
6·000	1·410	1·400	1·400	1·400	1·395	1·395	1·395
6·500	1·370	1·365	1·360	1·355	1·355	1·355	1·355
7·000	1·345	1·335	1·330	1·325	1·325	1·320	1·320
8·000	1·310	1·305	1·300	1·295	1·290	1·285	1·285
9·000	1·280	1·270	1·260	1·260	1·260	1·255	1·255
1·000*1	1·250	1·245	1·240	1·235	1·230	1·230	1·230
1·100*1	1·230	1·225	1·220	1·215	1·215	1·215	1·215
1·200*1	1·210	1·205	1·205	1·200	1·195	1·195	1·195
1·300*1	1·185	1·185	1·185	1·185	1·185	1·180	1·180
1·400*1	1·170	1·170	1·170	1·170	1·170	1·170	1·170

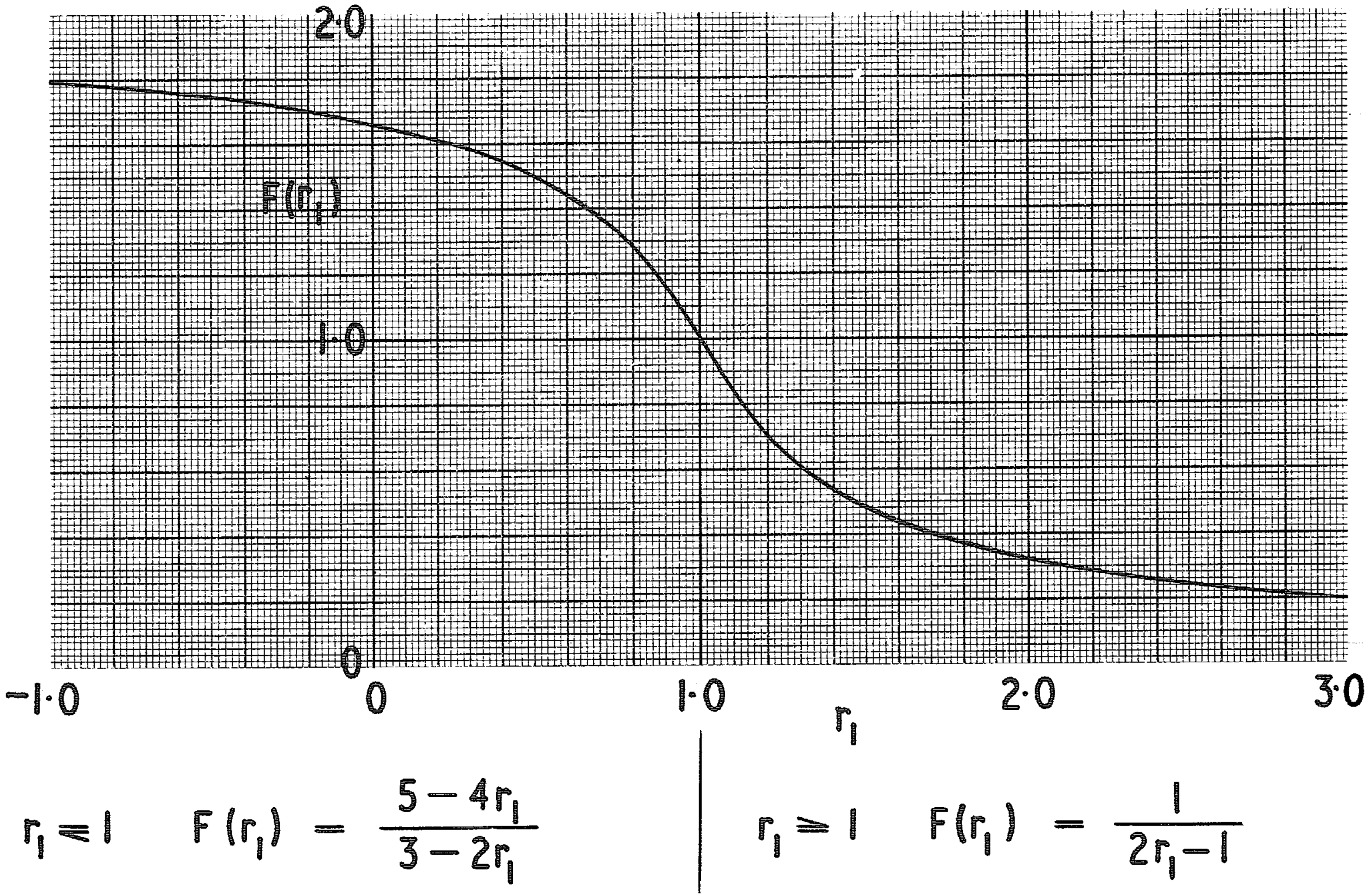

FIG. 1. The function $F(r_1)$.

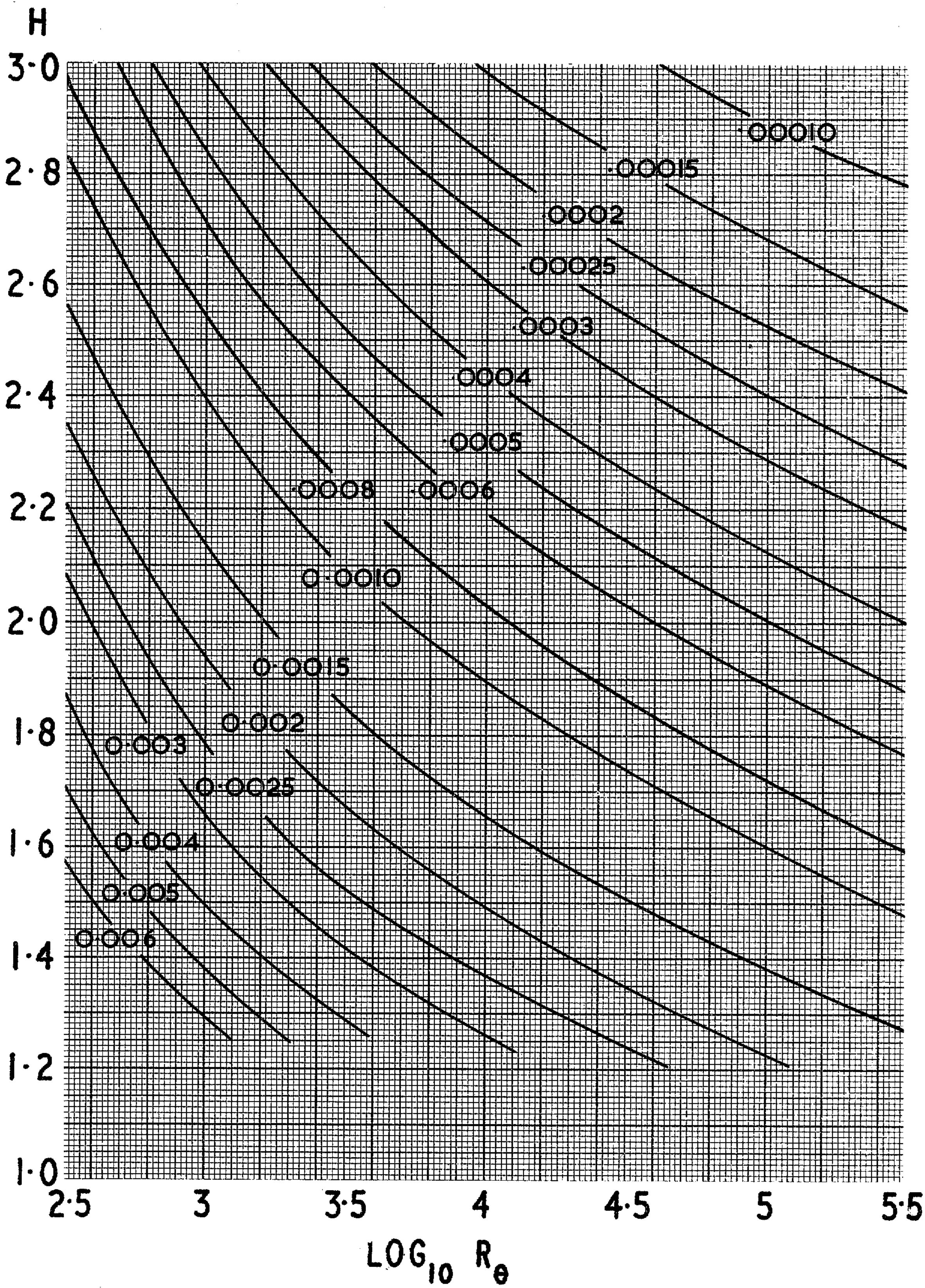

FIG. 2. $c_f(R_\theta, H)$.

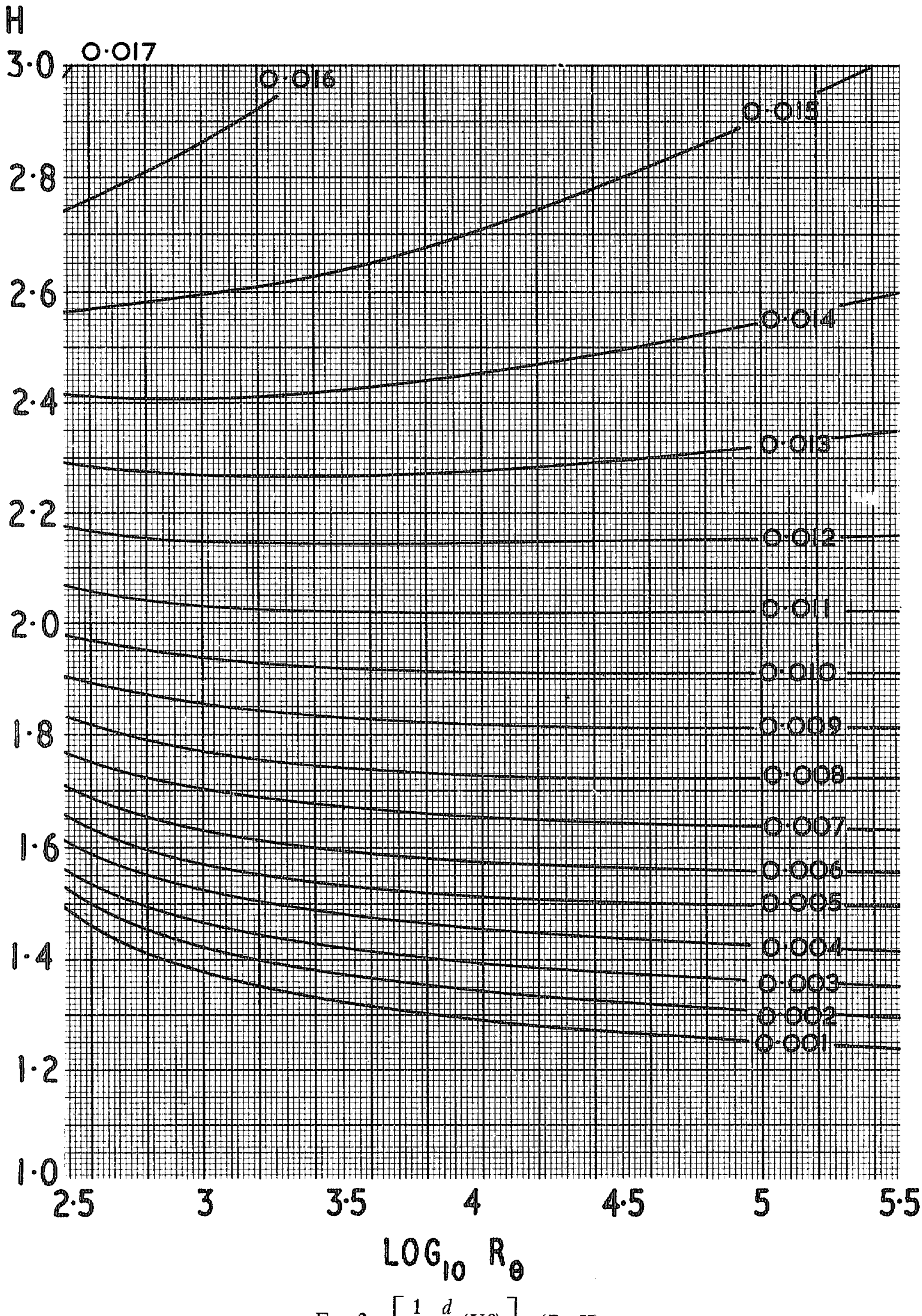

FIG. 3. $\left[\frac{1}{U}\frac{d}{dx}(U\theta)\right]_{eq}(R_\theta, H)$.

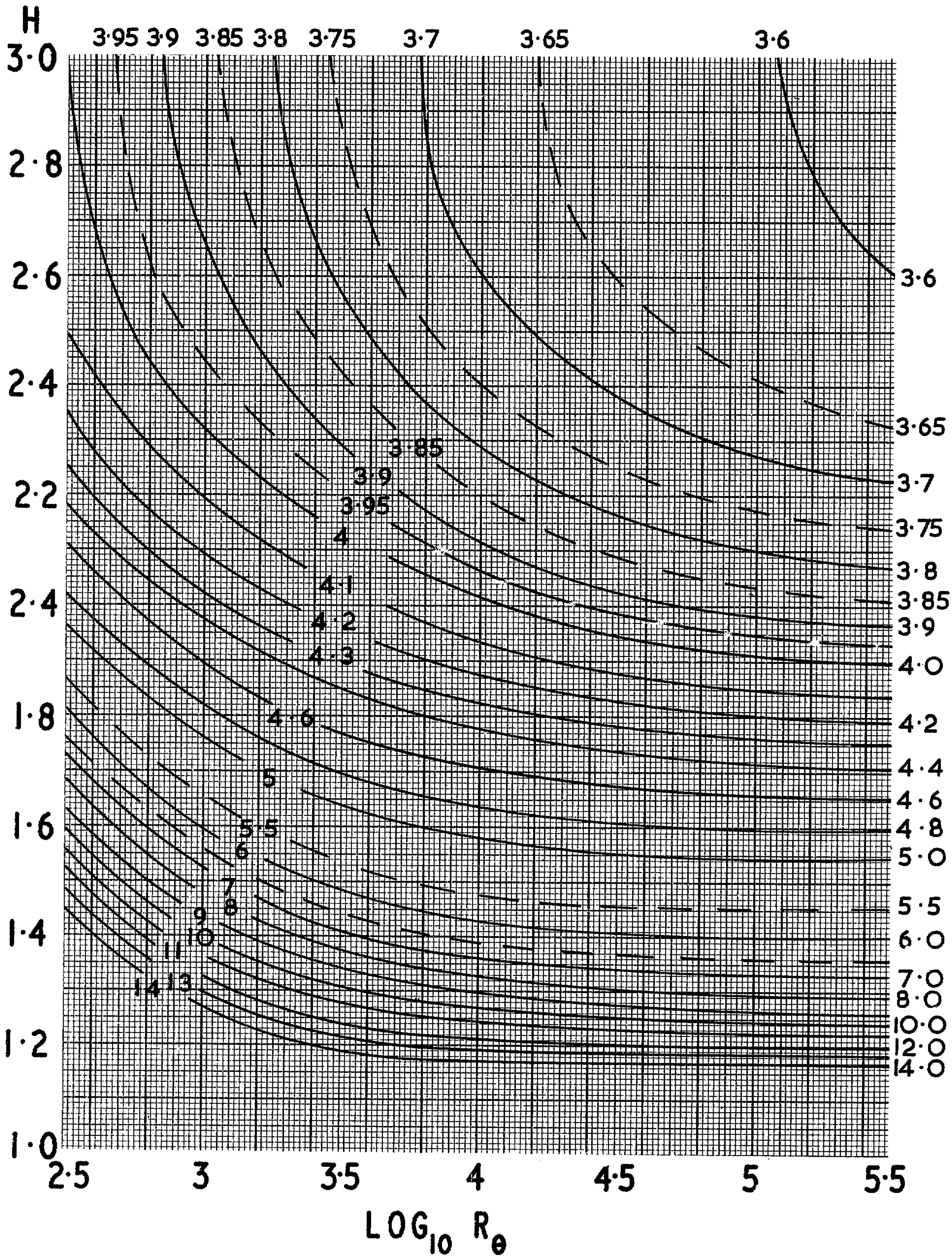

FIG. 4. $H^{*}(R_\theta, H)$.

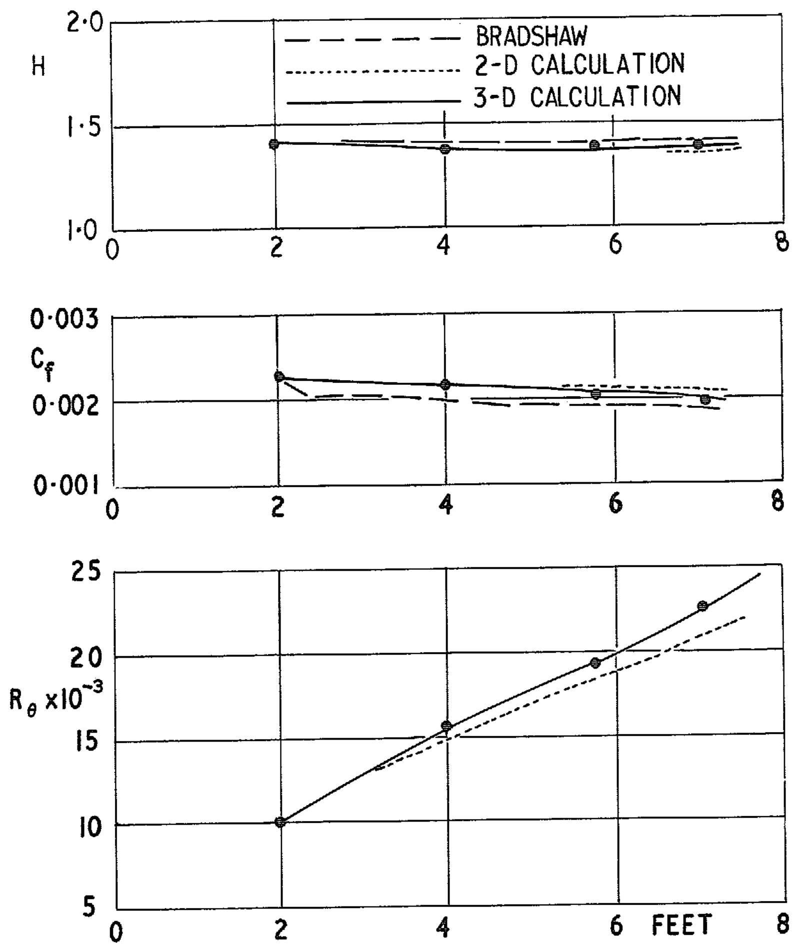

FIG. 5. Equilibrium flow measured by Bradshaw ($a = -0{\cdot}15$).

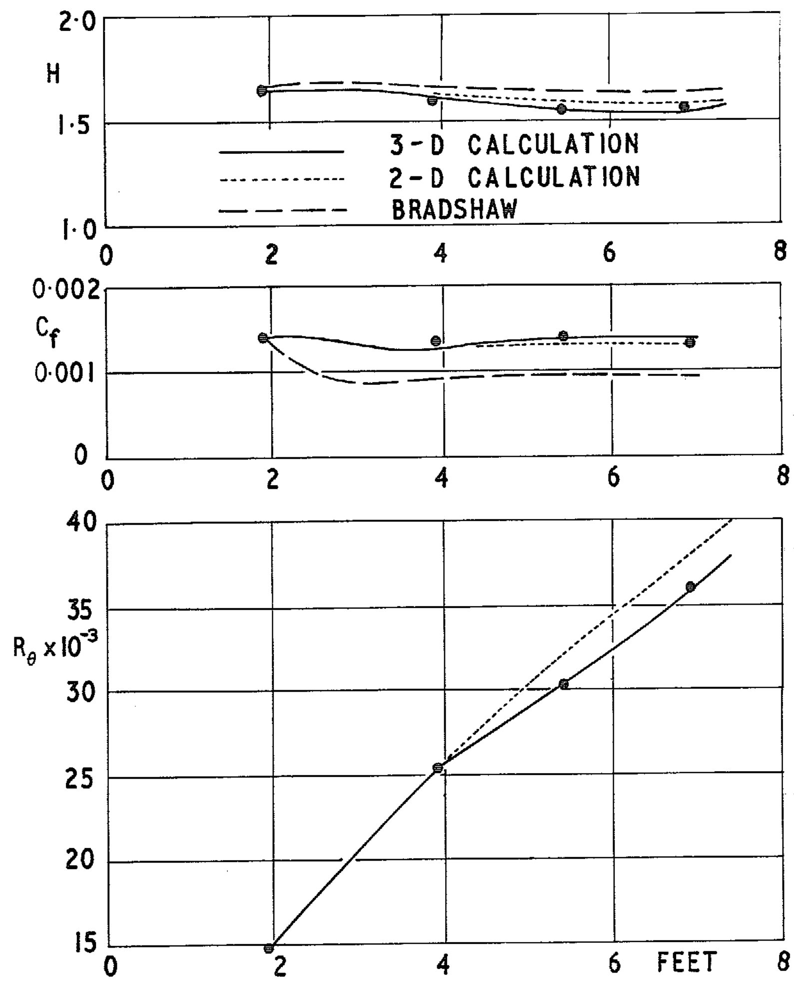

FIG. 6. Equilibrium flow measured by Bradshaw ($a = -0{\cdot}255$).

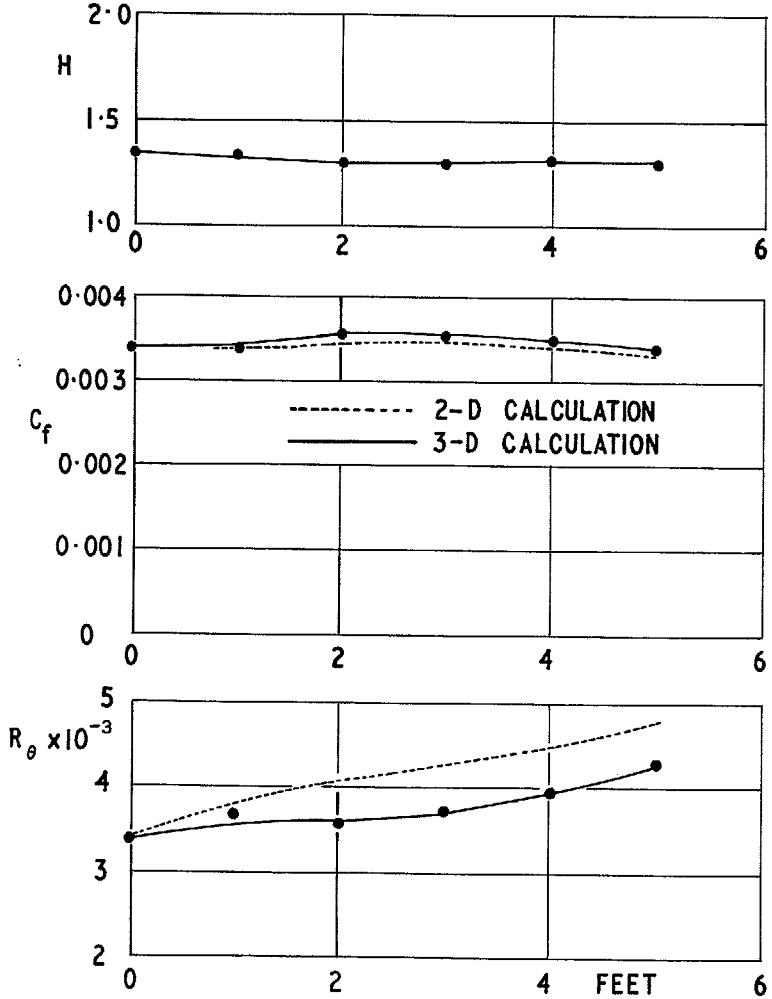

FIG. 7. Equilibrium flow measured by Herring and Norbury ($\beta = -0{\cdot}35$).

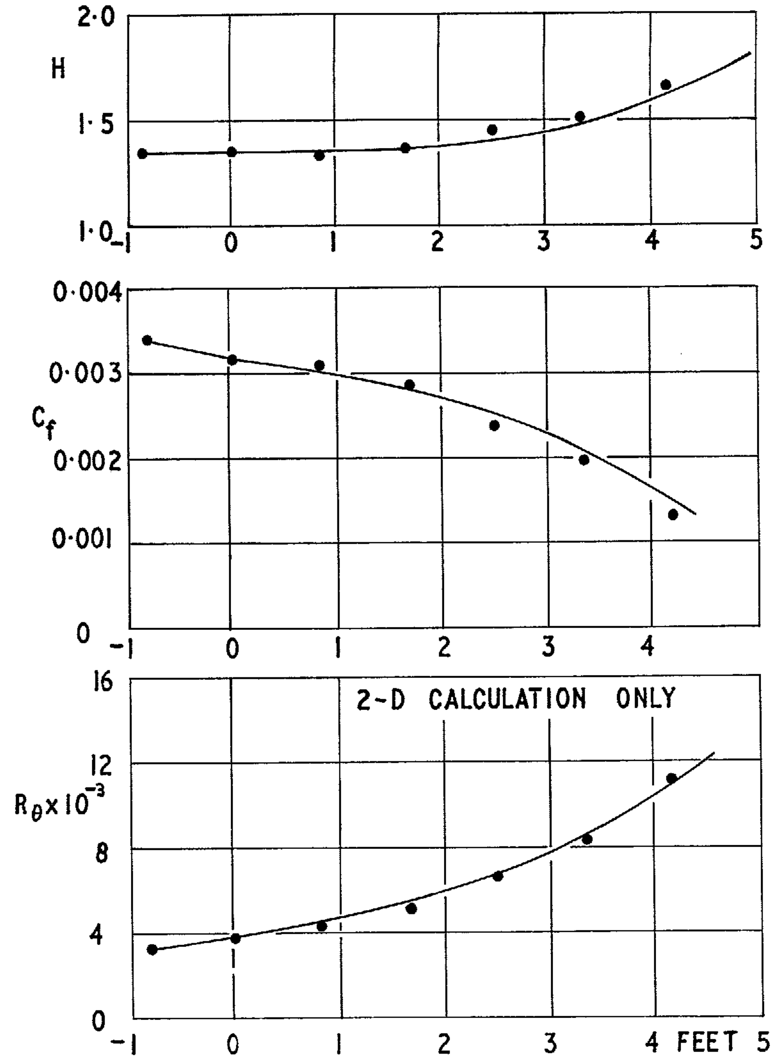

FIG. 8. Measurements by Schubauer and Spangenberg (flow A).

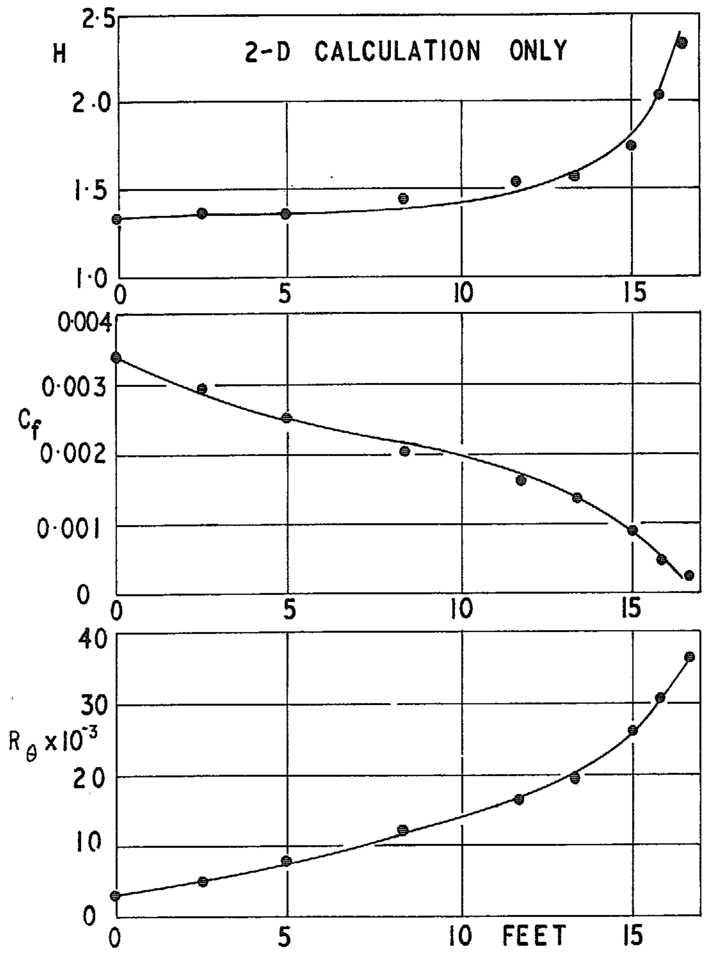

FIG. 9. Measurements of Schubauer and Spangenberg (flow *E*).

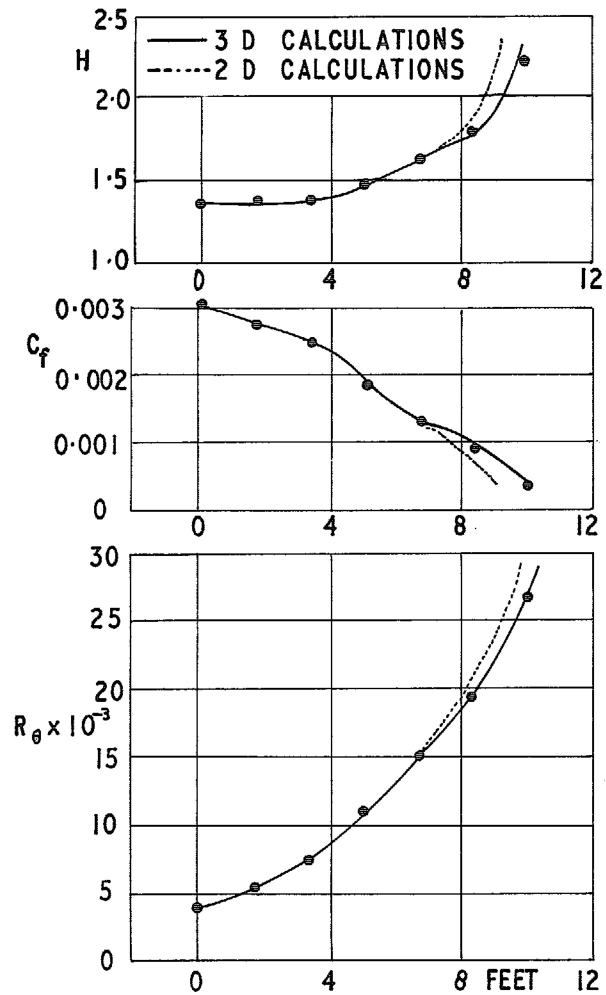

FIG. 10. Measurements by Schubauer and Spangenberg (flow *B*).

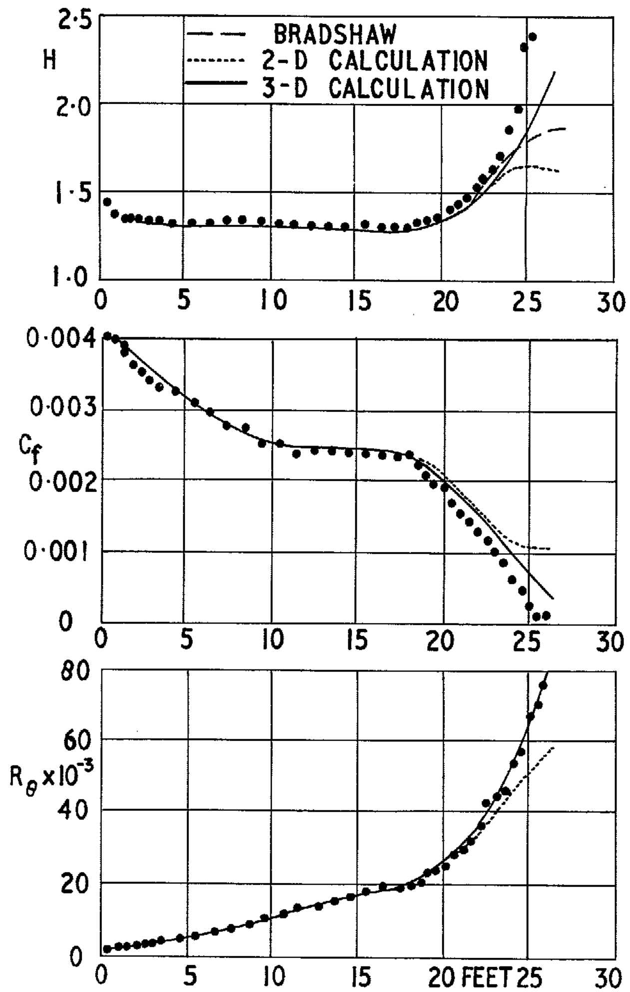

FIG. 11. Measurements of Schubauer and Klebanoff.

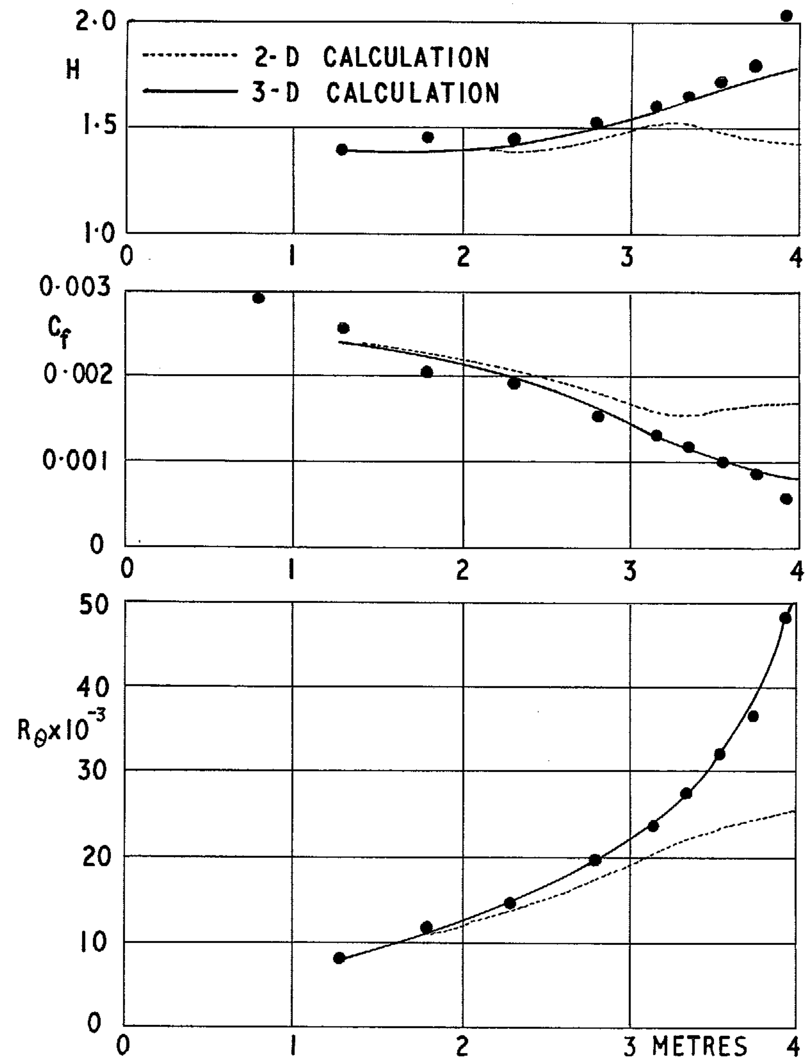

FIG. 12. Measurements by Ludwieg and Tillmann. (Strong adverse pressure gradient).

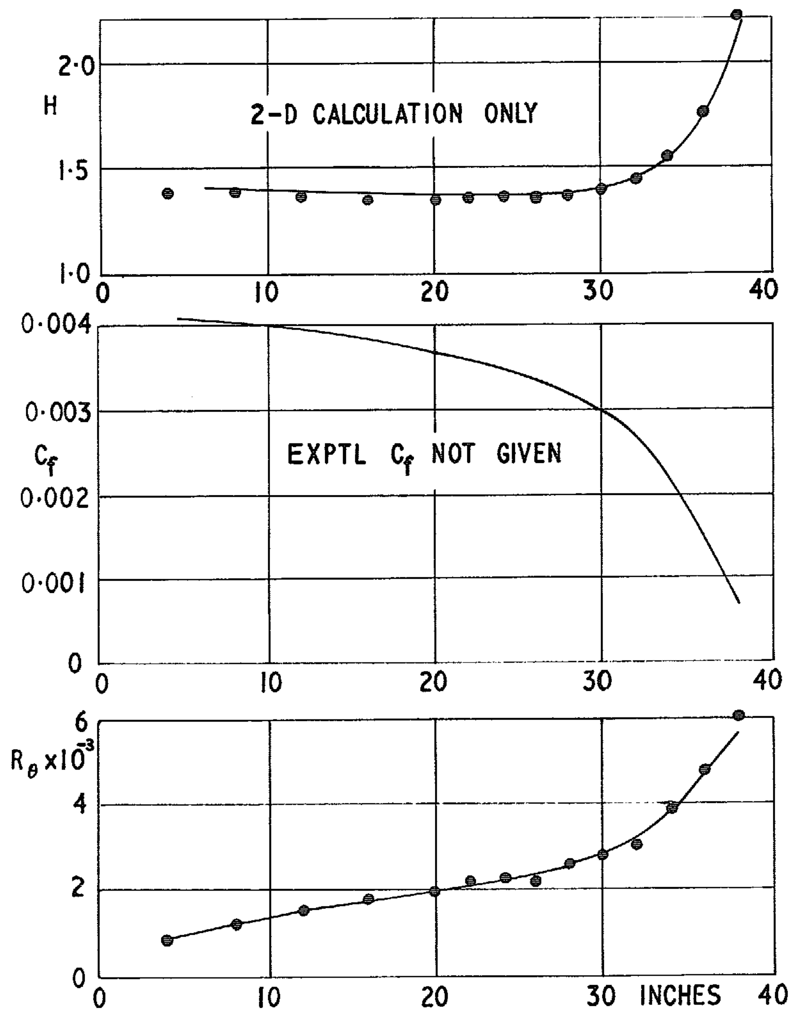

FIG. 13. Measurements by Goldberg. (Pressure distribution 6).

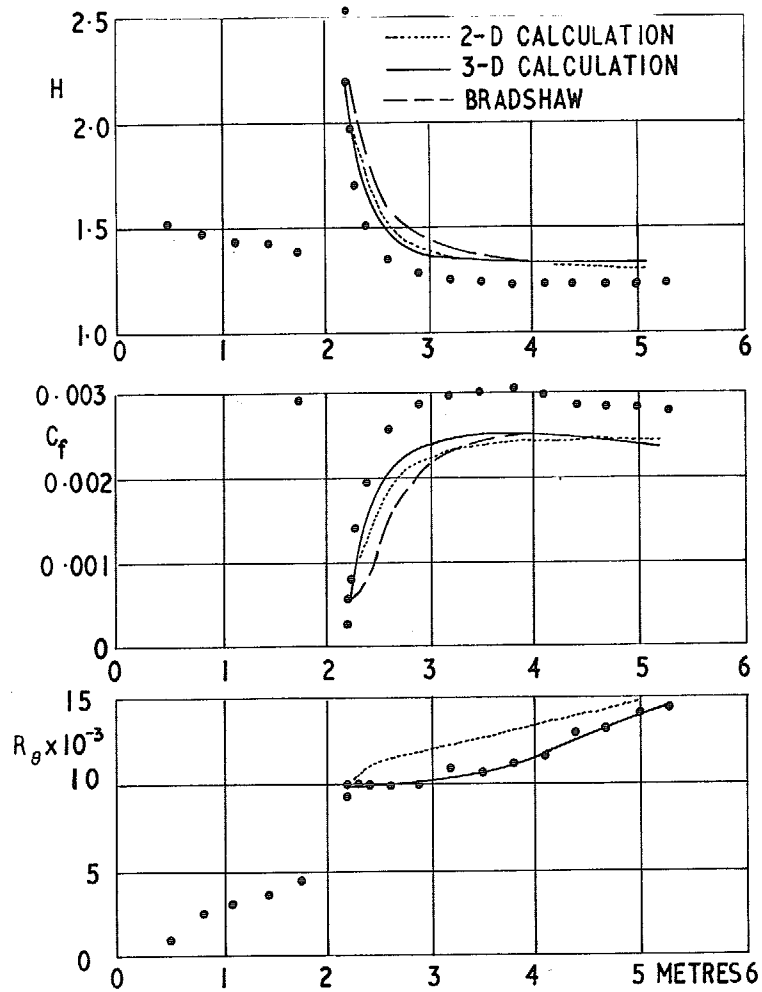

FIG. 14. Reattaching flow measured by Tillmann.

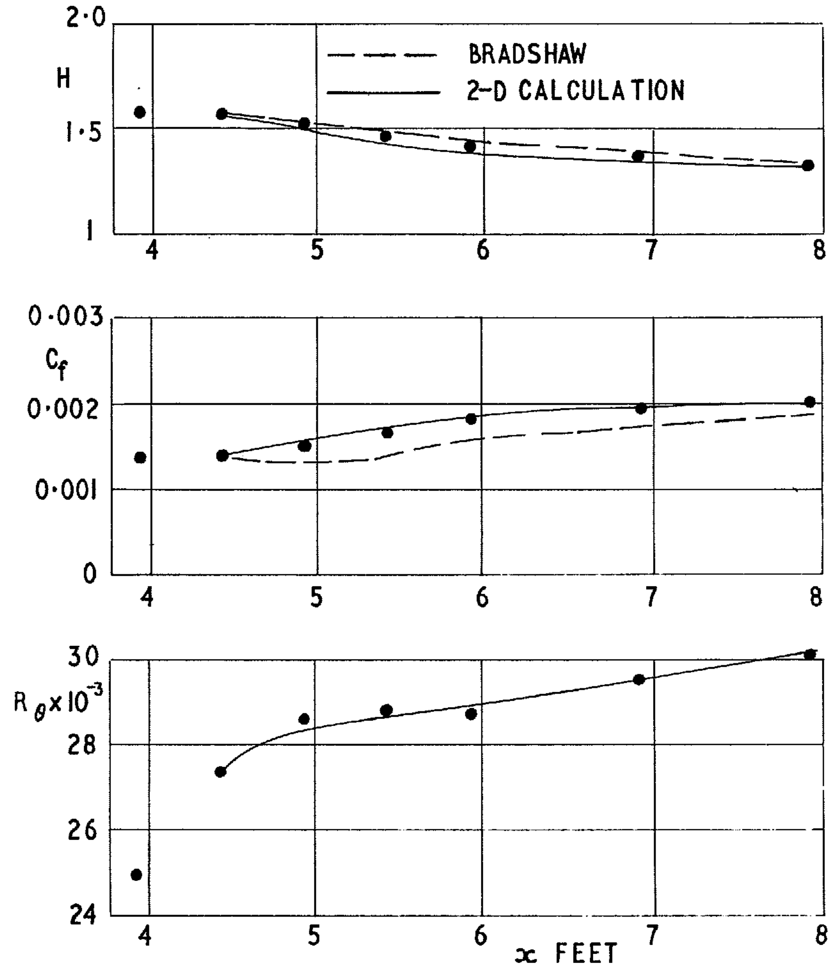

FIG. 15. Relaxing flow measured by Bradshaw.

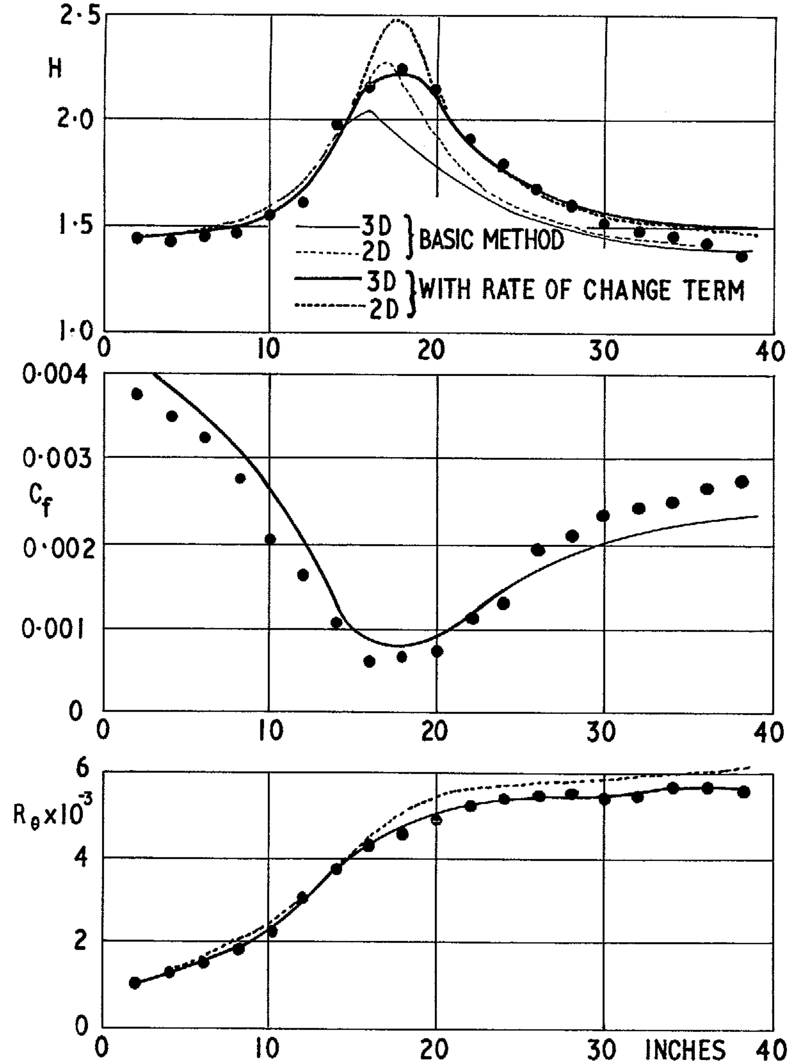

FIG. 16. Measurements by Goldberg.
(Pressure distribution 3).

Printed in Wales for Her Majesty's Stationery Office by Allens Printers (Wales) Limited
Dd. 501372 K.5

R. & M. No. 3643

© *Crown copyright* 1970

Published by
HER MAJESTY'S STATIONERY OFFICE

To be purchased from
49 High Holborn, London WC1 6HB
13a Castle Street, Edinburgh EH2 3AR
109 St Mary Street, Cardiff CF1 1JW
Brazennose Street, Manchester M60 8AS
50 Fairfax Street, Bristol BS1 3DE
258 Broad Street, Birmingham 1
7 Linenhall Street, Belfast BT2 8AY
or through any bookseller

R. & M. No. 3643
SBN 11 470363 9